Treg-targeted IL-2/anti-IL-2 complex controls graft-*versus*-host disease and supports anti-tumor effect in allogeneic hematopoietic stem cell transplantation

Allan Thiolat,[1*] Caroline Pilon,[1,2*] Pamela Caudana,[3,4] Audrey Moatti,[1] Nhu Hanh To,[1] Christine Sedlik,[3,4] Mathieu Leclerc[1,5] Sébastien Maury[1,2,5] Eliane Piaggio[3,4#] and José L Cohen[1,2#]

[1]University Paris Est Créteil, INSERM U955, IMRB, Créteil; [2]AP-HP, Groupe Hospitalo-Universitaire Chenevier Mondor, Centre d'Investigation Clinique Biothérapie, Fédération Hospitalo-Universitaire TRUE, Créteil; [3]INSERM U932, PSL Research University, Institute Curie Research Center, Paris; [4]Department of Translational Research, PSL Research University, Institute Curie Research Center, Paris and [5]AP-HP, Groupe Hospitalo-Universitaire Chenevier Mondor, Service d'Hématologie Clinique, Créteil, France

AT and CP contributed equally as first authors.

#EP and JLC contributed equally as senior authors.

Correspondence: J.L. Cohen
jose.cohen@inserm.fr

Received: January 6, 2023.
Accepted: September 7, 2023.
Early view: September 14, 2023.

https://doi.org/10.3324/haematol.2022.282653

Supplemental table 1. List of antibodies used

Antigens	Clones	Fluorochromes	Manufacturers
H2Kk	AF3-12.1.3	eF450	Invitrogen
H-2Kd	SF-1.1	PE	Invitrogen
CD3	145-2C11	PE-Cy5	Invitrogen
CD3	145-2C11	BV510	Invitrogen
CD8	REA601	FITC	Miltenyi
NKP46	29A1.4.9	PE	Miltenyi
CD62L	MEL-14	PE	Invitrogen
CD120b	REA228	APC	Miltenyi
CD44	REA664	APC-Cy7	Invitrogen
CD4	RM4-5	PE-Cy	Invitrogen
CD4	RM4-5	APC-Cy7	Invitrogen
PD-1	HA2-7B1	V450	Miltenyi
CD25	PC61,5	PE-Cy7	Invitrogen
CD44	IM7	PE-Cy7	Invitrogen
CD4 (hu)	RPA-T4	APC	BD Biosciences
CD4 (hu)	RPA-T4	PerCP-Cy5.5	BD Biosciences
CD4 (hu)	RPA-T4	APC-Cy7	BD Biosciences
CD8 (hu)	RPA-T8	PE	BD Biosciences
CD56 (hu)	B159	APC	BD Biosciences
CD45 (hu)	HI30	APC	BD Biosciences
CD25	2A3	PE-Cy7	BD Biosciences

INTRACELLULAR

Antigens	Clones	Fluorochromes	Manufacturers
Foxp3	FJK-16S	eF450	Invitrogen
Foxp3	FJK-16S	PE-Cy5	Invitrogen
TBET	30F11	APC	Miltenyi
CTLA-4	UC10-4B9	PE	Invitrogen
EOMES	REA116	PE	Miltenyi
TNFa	REA636	FITC	Miltenyi
INFg	REA638	PE	Miltenyi
IL-17	TC-11,18H10	APC	Miltenyi
Foxp3 (hu)	PCH101	eF450	Invitrogen
Ki67	B56	FITC	BD Biosciences

VIABILITY

	Fluorochromes	Manufacturers
Fixable viability stain	AF R700	BD Biosciences
Fixable viability dye	V500	Invitrogen

Supplemental figure 1

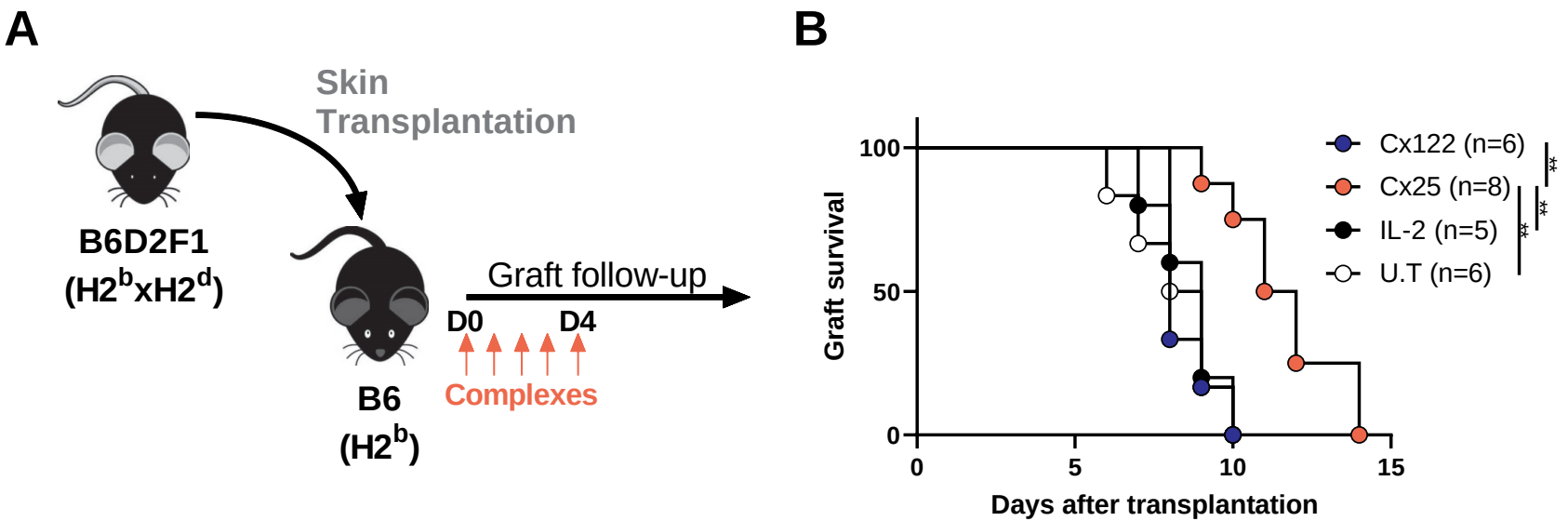

Only Cx25 prolongs allogeneic skin transplantation.

(**A**) B6 recipient mice were grafted with skin from B6D2F1 donor mice. Grafted mice were divided into four groups: untreated (n=6), IL-2 alone (n=5), Cx25 alone (n=8) and Cx122 alone (n=6), (**B**) Graft survival curves of cumulative data of two independent experiments are shown. Kaplan Meier survival curves were compared using the log-rank test. *P < 0.05, **P < 0.01, ***P < 0.001.

Supplemental figure 2

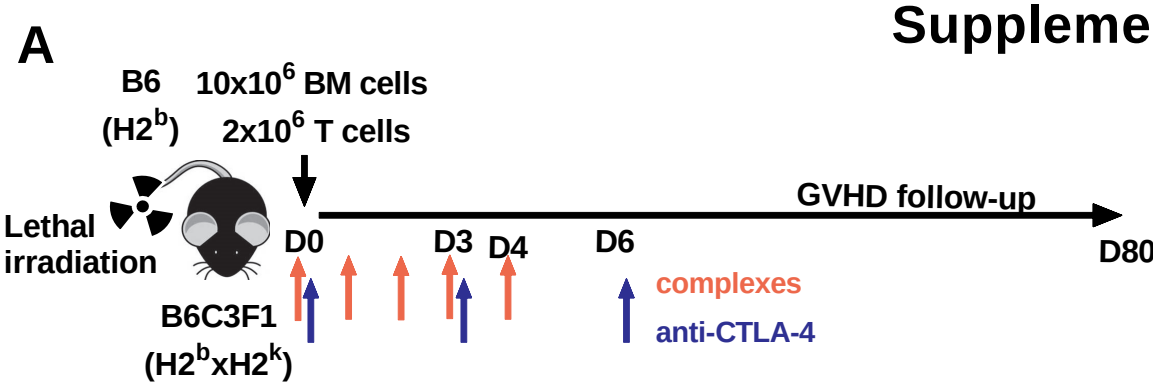

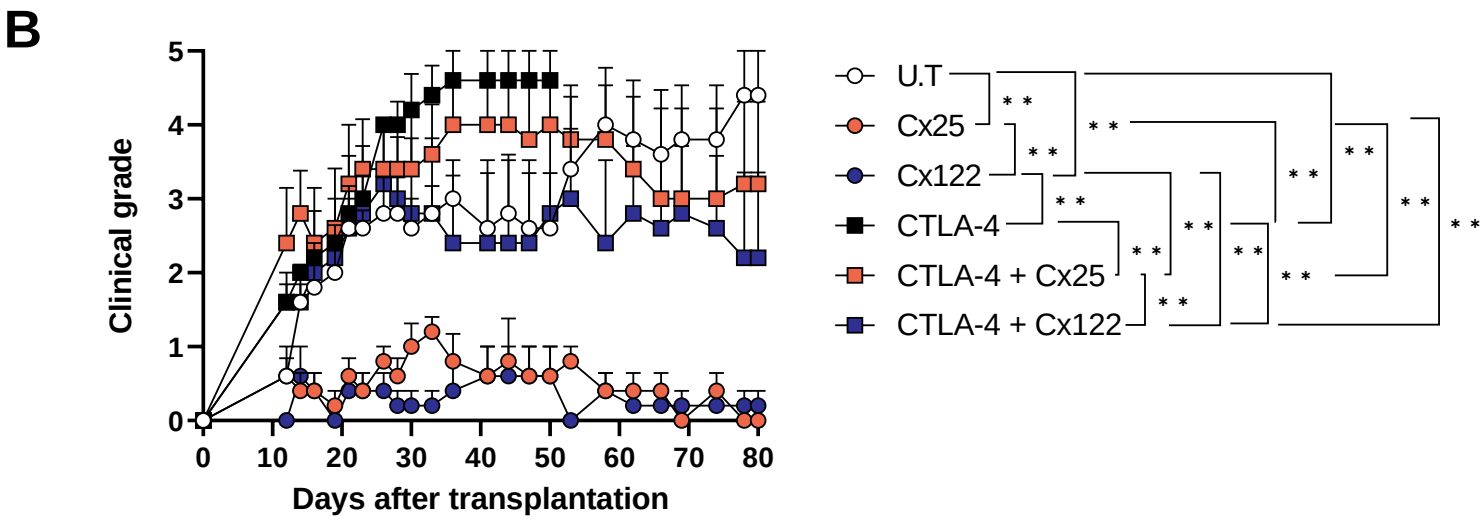

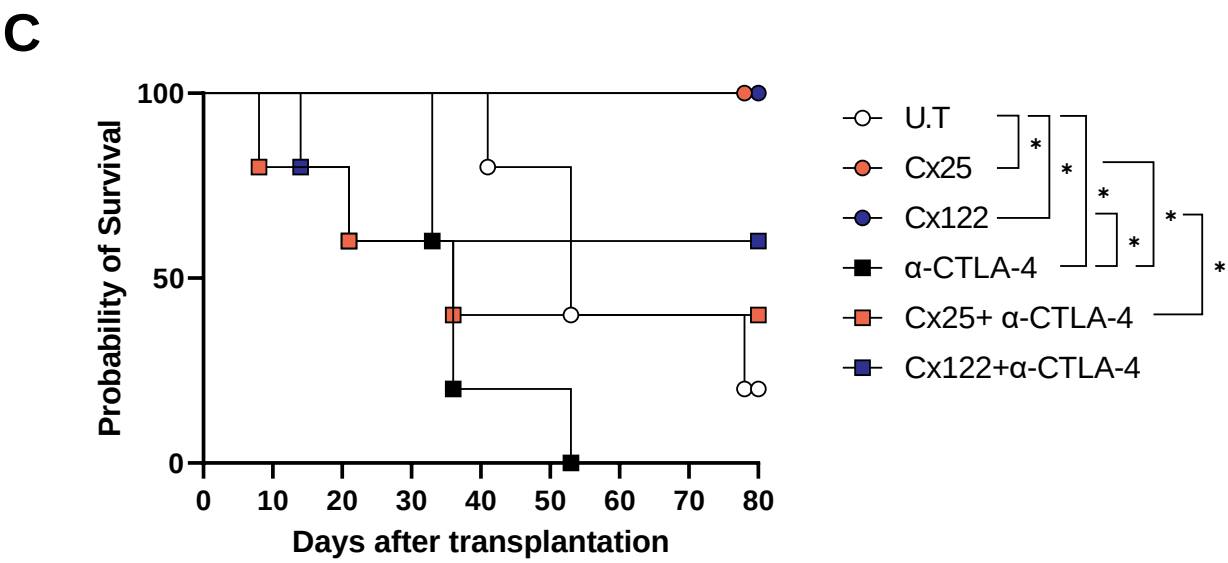

Anti-CTLA4 inhibits IL-2Cx-mediated GVHD prevention.

(**A**) Lethally irradiated B6C3F1 received semi-allogeneic HSCT (10 x 10^6 BM cells plus 2 x 10^6 T cells). Mice were untreated (n=5) or treated from d0 to d4 after HSCT with Cx25 (n=5), Cx122 (n=5), anti-CTLA4 (n=5), Cx25 + anti-CTLA4 (n=5) or Cx122 + anti-CTLA4 (n=5). (**B**) Clinical grade curves were compared using two-way Anova test. (**C**) Kaplan Meier survival curves were compared using the log-rank test. *P < 0.05, **P < 0.01

Supplemental figure 3

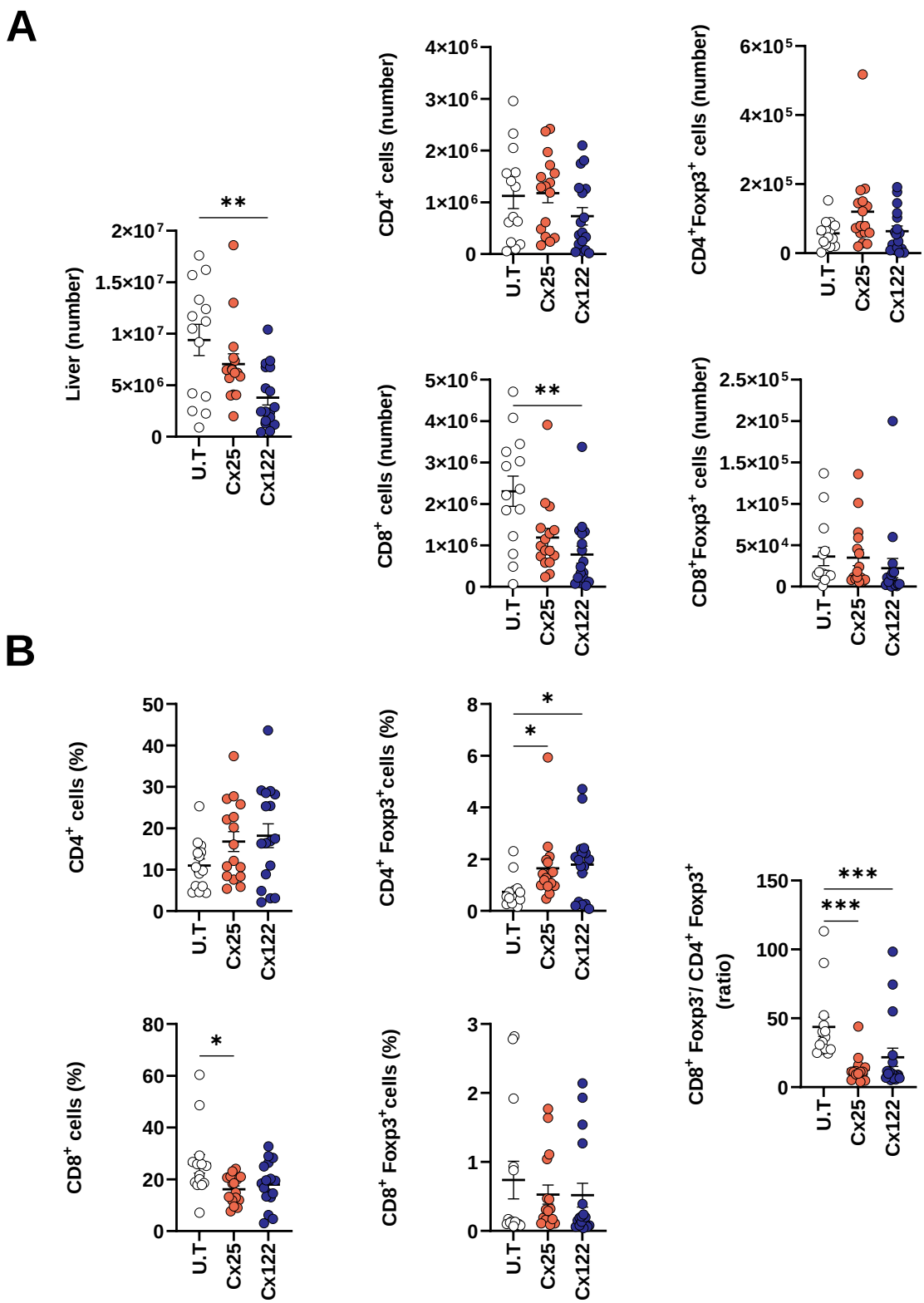

IL-2/anti-IL-2 complexes modify the CD8+Foxp3-/CD4+Foxp3+ ratios in the liver of grafted animals.

Lethally irradiated B6C3F1 received 10 x 106 semi-allogeneic B6 BM cells and 2 x 106 B6 T cells and were treated as for Figure 2. On d12, mice were sacrificed and livers were collected for analysis. (**A**) Numbers of liver cells and CD4+ and CD8+ T cells are depicted as in figure 3A. (**B**) Percentages of CD4+Foxp3-, CD4+Foxp3+, CD8+Foxp3- and CD8+Foxp3+ cells among live liver cells and CD8+Foxp3-/ CD4+Foxp3+ ratios are shown for each group of mice as in Figure 3A. Data cumulative from three independent experiments are presented as the mean ± SEM. Kruskal-Wallis tests were performed. *P < 0.05, **P < 0.01, ***P<0.001.

Supplemental figure 4

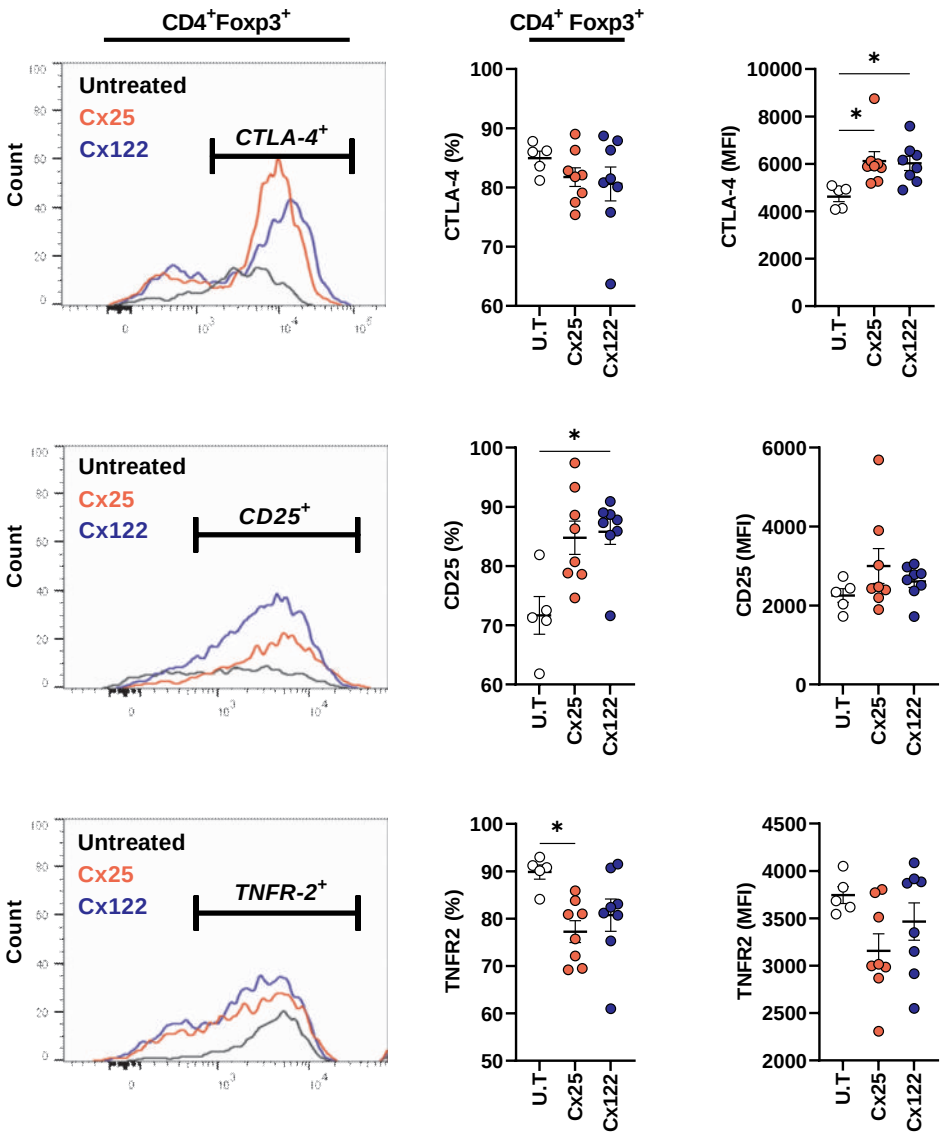

Effects of Cx25 or Cx122 treatment on regulatory T cell phenotype.

B6C3F1 mice were lethally irradiated and grafted and were either untreated (n=5) or treated from d0 to d4 after HSCT with Cx25 (n=8) or with Cx122 (n=8). On d12, mice were sacrificed and the percentages and MFI values of CTLA-4+, TNFR2+ and CD25+ among regulatory T cells defined as CD4+ Foxp3+ cells were analyzed by flow cytometry. Histogram staining, percentage and MFI value of CTLA-4+, TNFR2+ and CD25+ among CD4+Foxp3+ cells are shown for each group. Data are the cumulative data of two independent experiments. Data are presented as the mean ± SEM. Kruskal-Wallis tests were performed to compare each group. *P < 0.05.

Supplemental figure 5

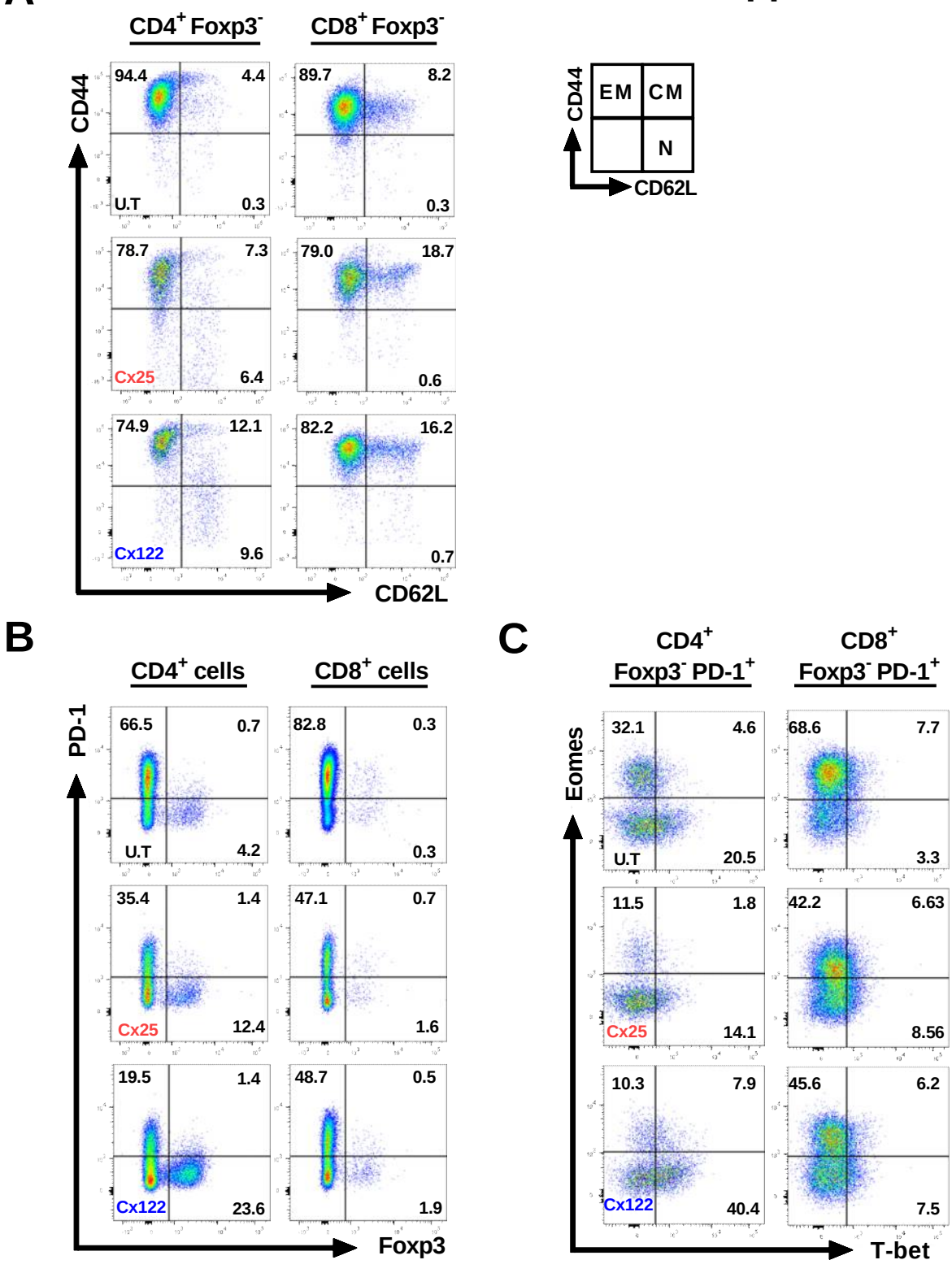

IL-2/anti-IL-2 complexes modify the distribution of naïve/memory populations and the activation state of T cells after HSCT.

B6C3F1 mice were lethally irradiated and grafted as for figures 2 and 3 and were either untreated (n=8) or treated from d0 to d4 after HSCT with Cx25 (n=7) or with Cx122 (n=8). On d12, mice were sacrificed and memory, effector and naïve T cells were analyzed from splenocytes of grafted animals by flow cytometry. Gating strategy of (**A**) effector memory (defined as $CD44^+$ $CD62L^-$ cells), central memory (defined as $CD44^+CD62L^+$ cells), and naïve (defined as $CD44^-$ $CD62L^+$ cells) cells, among $CD4^+Foxp3^-$ cells and $CD8^+Foxp3^-$cells are shown for each group (**B**) PD-1 among $CD4^+$ and $CD8^+$ T cells according to Foxp3 expression and (**C**) Eomes and T-bet among $CD4^+Foxp3^-PD\text{-}1^+$ and $CD8^+Foxp3^-PD1^+$ T cells analyzed by flow cytometry.

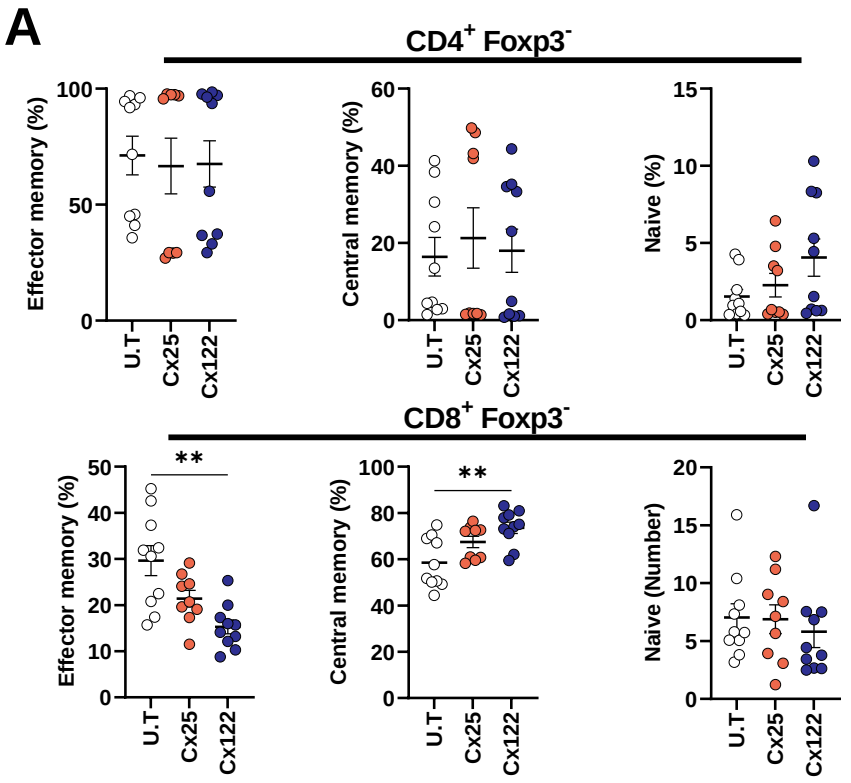

Supplemental figure 6

IL-2/anti-IL-2 complexes effects on the distribution of naïve/memory cell populations and on the activation state of T cells collected from livers of transplanted animals.

B6C3F1 mice were lethally irradiated and grafted as for Figure 2 and were either untreated or treated from d0 to d4 after HSCT with Cx25 or with Cx122. On d12, mice were sacrificed and memory, effector and naïve T cells were analyzed from livers of grafted animals by flow cytometry. (**A**) Percentage of effector memory (defined as CD44+ CD62L- cells), central memory (defined as CD44+ CD62L+ cells), and naïve (defined as CD44- CD62L+ cells) cells, among CD4+Foxp3- cells, and CD8+Foxp3- cells are shown for each group; untreated mice (n=10), Cx25 (n=9) and Cx122 (n=10). (**B**) PD-1 among CD4+ and CD8+ T cells according to Foxp3 expression and (**C**) Eomes and T-bet expression among CD4+Foxp3-PD-1+ and CD8+Foxp3-PD1+ T cells were also analyzed. Shown are the cumulative data of two independent experiments; untreated mice (n=5), Cx25 (n=8) and Cx122 (n=8). Data are presented as the mean ± SEM. Kruskal-Wallis tests were performed. *P < 0.05, **P < 0.01, ***P < 0.001.

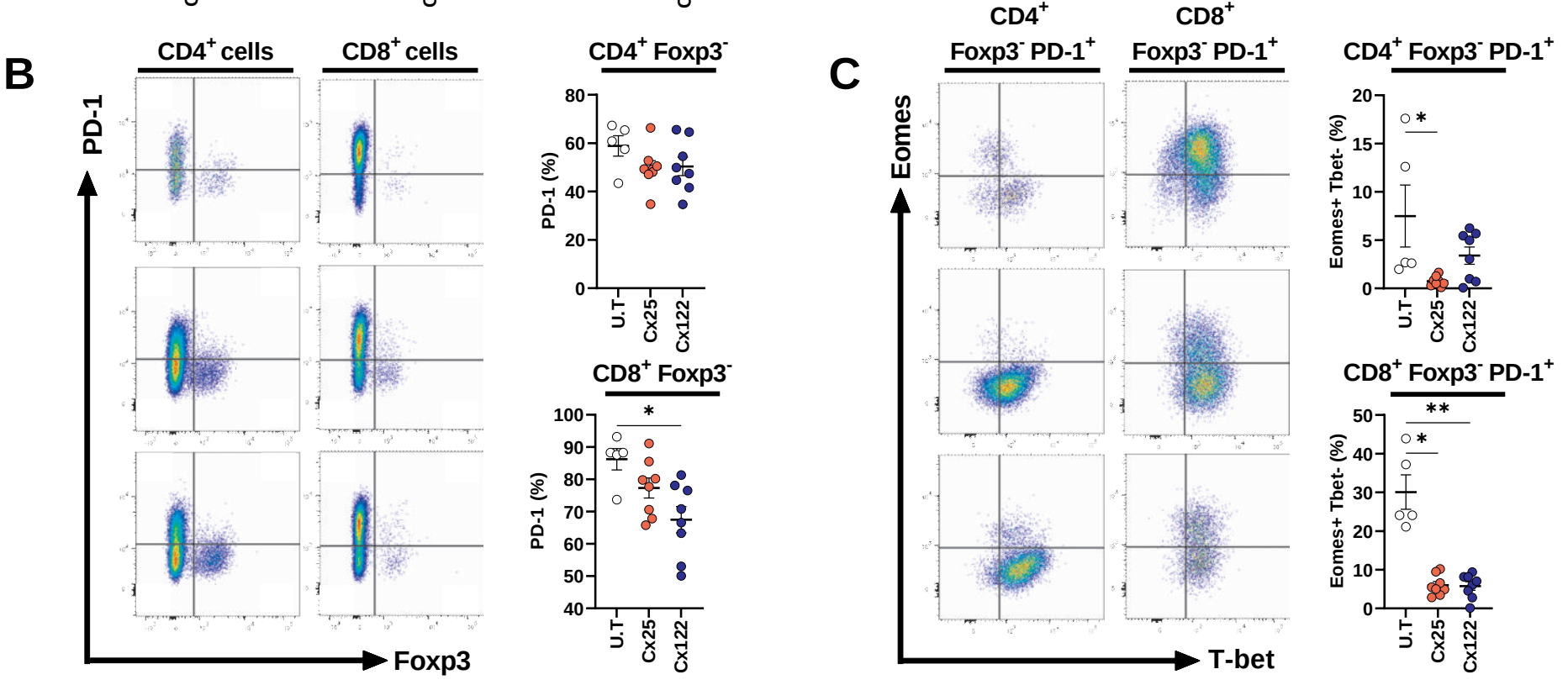

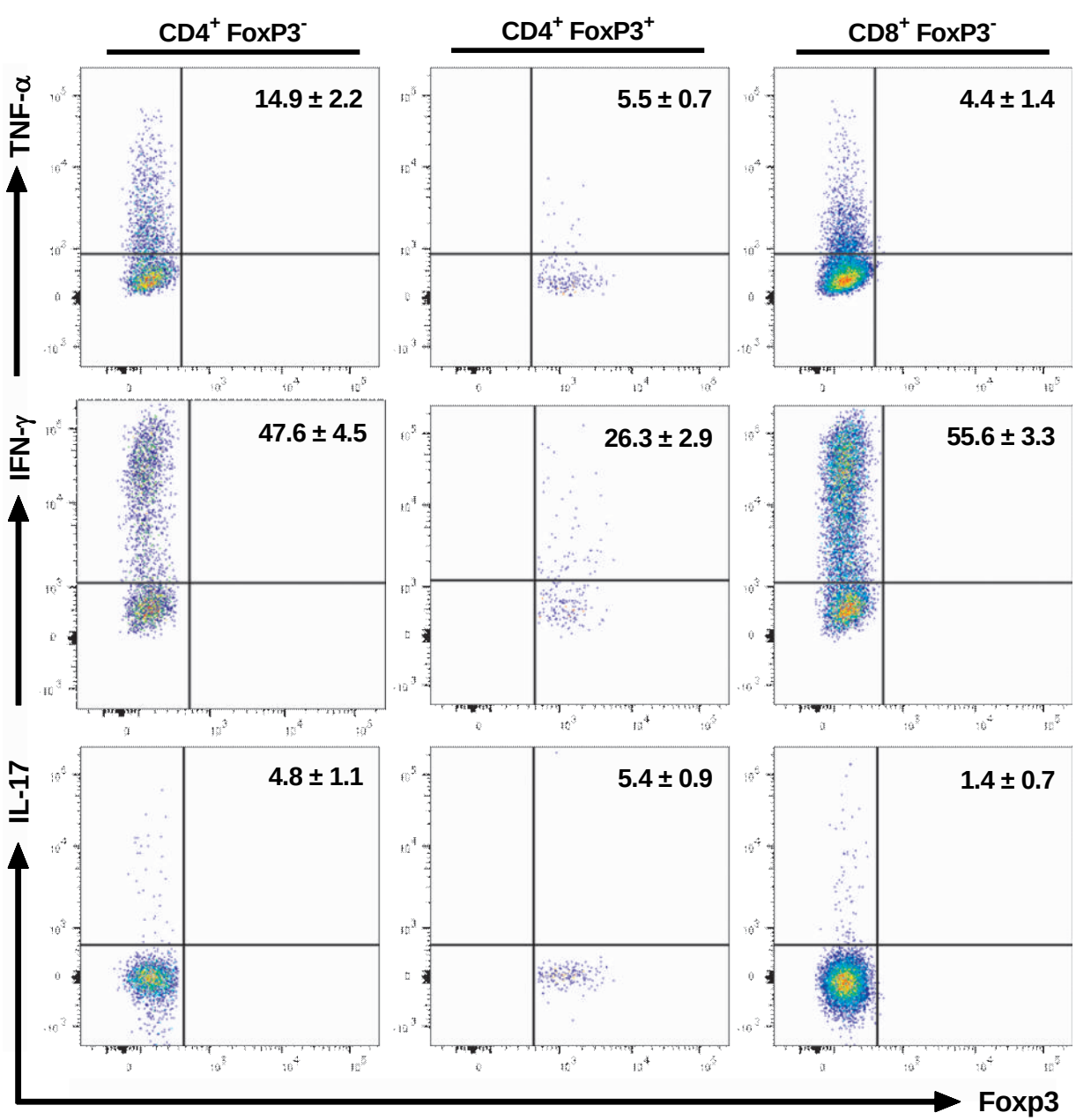

Supplemental figure 7

IL-2/anti-IL-2 complexes inhibit pro-inflammatory cytokines production by regulatory T cells after HSCT.

B6C3F1 mice were lethally irradiated and grafted as for figures 2 and 3 and were either untreated (n=14) or treated from d0 to d4 after HSCT with Cx25 (n=16) or with Cx122 (n=17). On d12, mice were sacrificed and splenocytes were collected and then stimulated with PMA/ionomycin and golgi plug for 5 hours before analysis by flow cytometry. Gating strategy of TNF-α, IFN-γ and IL-17 expression in CD4+Foxp3-, CD4+Foxp3+ and CD8+Foxp3- T cells analyzed by flow cytometry.

Supplemental figure 8

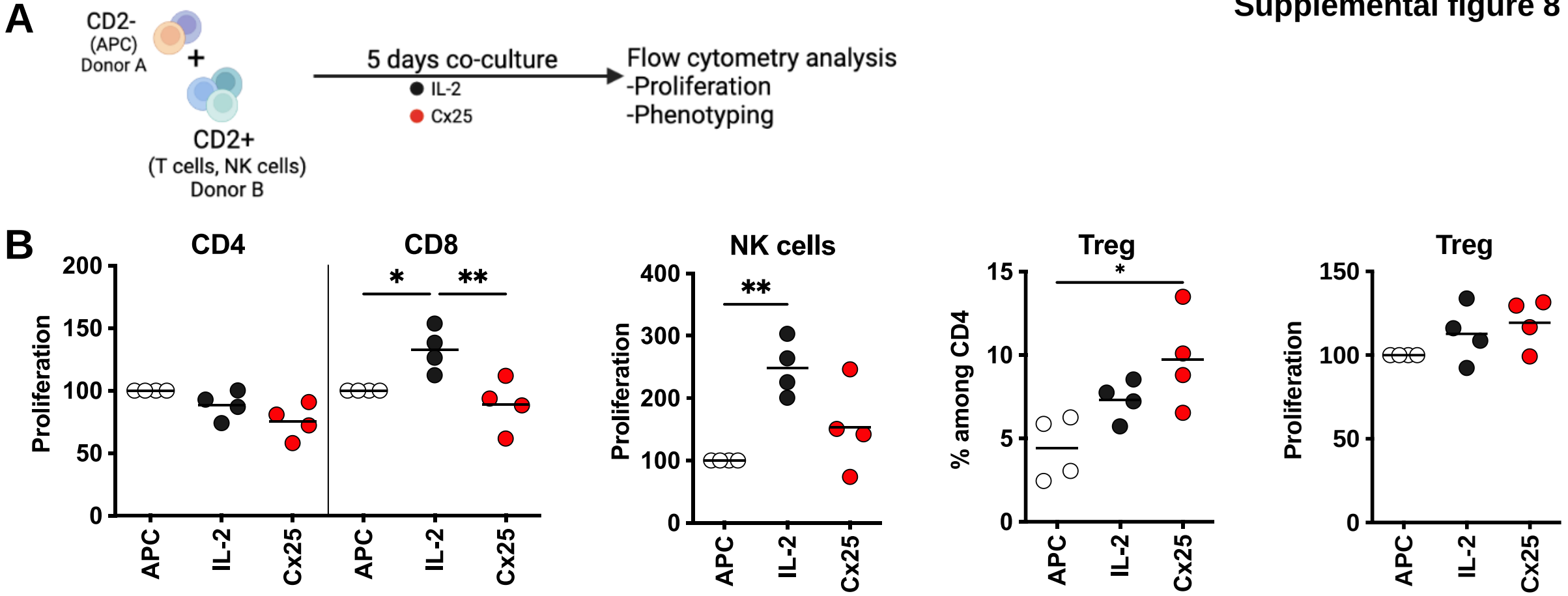

Cx25 induces human Treg expansion in vitro after an allogeneic stimulation.

(**A**) 1 x 10^6 $CD2^+$ sorted cells were stained with the cell proliferation dye and cultured with 1x10^6 allogeneic APCs ($CD2^-$ sorted cells) in the presence of IL-2 or Cx25. (**B**) At day 5, $CD4^+$, $CD8^+$ T cells, $CD56^+$ NK cell and Treg proliferations were evaluated in both $CD4^+$ and $CD8^+$ T cells and in NK cells. Treg proportion is defined by $CD25^+Foxp3^+$ expression among $CD4^+$ T cells. Dot blot sum the data of two independent experiments. Kruskal-Wallis tests were performed. *P < 0.05, **P < 0.01.

Supplemental figure 9

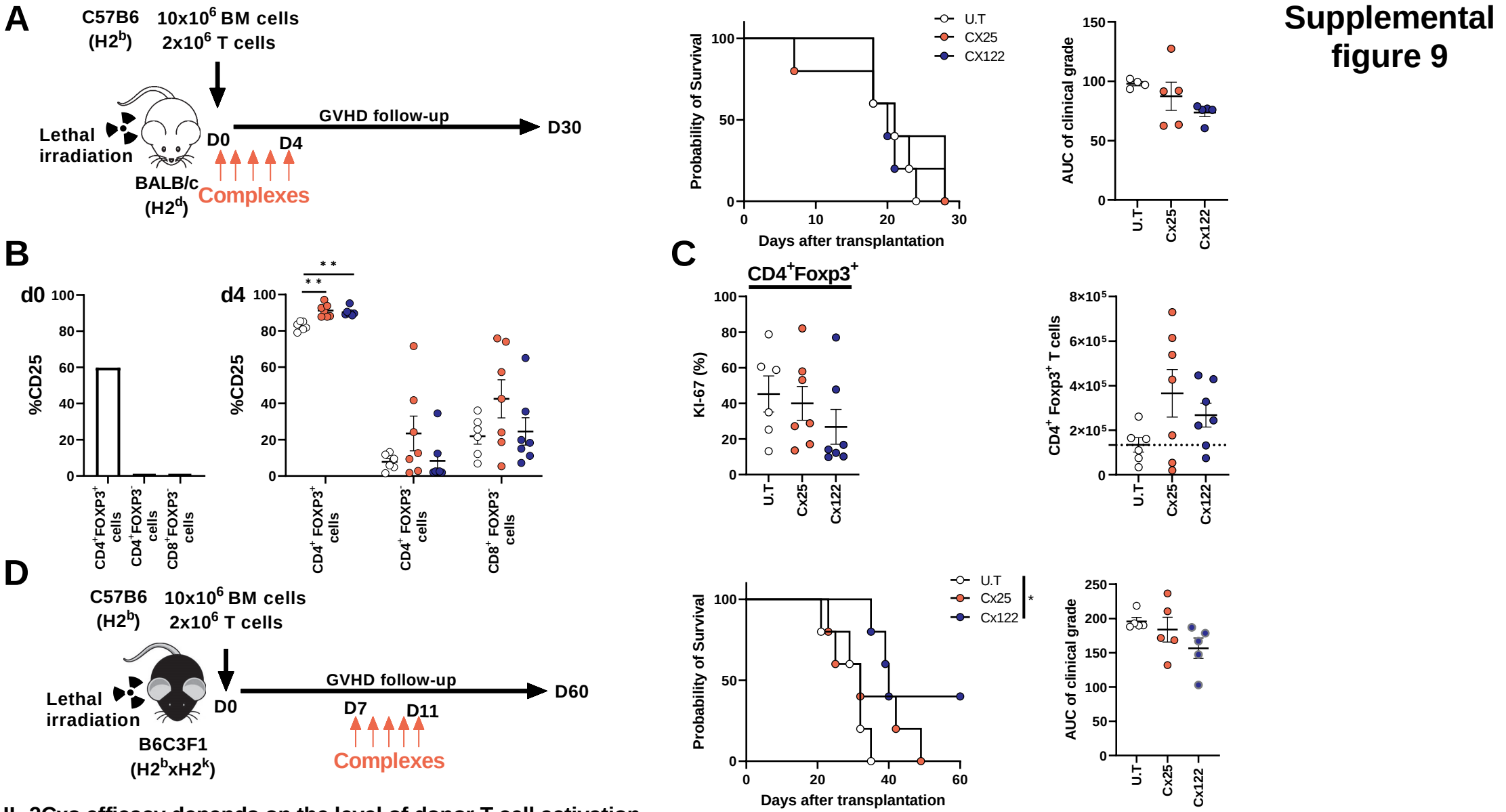

IL-2Cxs efficacy depends on the level of donor T cell activation.

(**A**) Lethally irradiated BALB/c mice received allogeneic HSCT (10 x 10^6 BM cells plus 2 x 10^6 T cells) collected from B6 mice. Mice were untreated (n=4) or treated from d0 to d4 after HSCT with Cx25 (n=5) or with Cx122 (n=5). Survival curves (left) and area under the curve (AUC) of GVHD manifestations are evaluated for each mouse for all the duration of the experiment as for Figure 1. (**B** and **C**) Lethally irradiated B6C3F1 received semi-allogeneic HSCT (10 x 10^6 BM cells plus 2 x 10^6 T cells) as in Figure 1. Before infusion, CD25 expression was assessed on donor T cells (left). Mice were sacrificed at d4, spleen cells were collected and evaluated for CD25 expression on T cells; untreated mice (n=6), Cx25 (n=7) and Cx122 (n=7). (**D**) Lethally irradiated B6C3F1 received semi-allogeneic HSCT (10 x 10^6 BM cells plus 2 x 10^6 T cells) as in Figure 1. Mice were untreated (n=5) or treated from d7 to d11 after HSCT with Cx25 (n=5) or with Cx122 (n=5).